

# DETECTION OF SPLENOMEGALY IN POULTRY CARCASSES BY UV AND COLOR IMAGING

Y. Tao, J. Shao, K. Skeeles, Y. R. Chen

**ABSTRACT.** *Splenomegaly (spleen enlargement) is one indication that processed poultry is not acceptable for human consumption because of diseases such as tumors or septicemia. This study explored the possibility of detecting splenomegaly with a computer imaging system that will assist human inspectors in food safety inspections. Images of internal viscera from 45-day-old commercial turkeys were taken with fluorescent and UV lighting systems. Image processing algorithms using the linear transformation, morphological filtering, and statistical classification were developed to distinguish the spleen from its background surroundings and then to detect abnormalities. Experimental results demonstrated that the imaging method could effectively distinguish the spleen from other organs and intestines. Based on a total of 57 turkey sample images, correct classification rates of 92% and 95% in detection of spleen abnormality were obtained using a self test set and an independent test set, respectively. The methods indicated the feasibility of using automated machine vision systems in the future to inspect internal organs and check the wholesomeness of poultry carcasses.*

**Keywords.** *Machine vision, Poultry, Automated inspection, Food safety, Disease detection, Spectral imaging.*

Poultry spleen size is one important indicator of whether the poultry is to be condemned and must be further examined by human inspectors in processing plants. According to poultry pathologists and veterinarians, if a chicken has an enlarged spleen, it is sure that the chicken is diseased (Schat, 1981; Clarke et al., 1990; Arp, 1982). Conversely, if a chicken has disease(s), the spleen is likely to be enlarged. As a part of the research on inspection of poultry carcasses for internal diseases, checking spleens using machine vision was suggested as an initial step. This will add to the further inspections for other disease syndromes such as Air Sacculitis and Inflammatory Process (Domermuth et al., 1978).

Inspection of poultry carcasses for wholesomeness or disease is a complex process. Developers of automated machine vision inspection technology must incorporate human knowledge into computer systems with machine intelligence. The development of such a vision system is often a progressive process, with problems conquered one at a time. Recently, substantial progress has been made on the machine vision inspection of poultry carcasses (Chen et al., 1998; Park et al., 1996). An on-line vision system was developed for inspecting for tumors, diseases, and abnormal items such as skin damage (Vision, 1998). With this system, external chicken surfaces were analyzed

through multi-spectral imaging and fiber optics. The system achieved sorting accuracies comparable to human sorting. The system seemed highly promising for detecting specific poultry disease problems, and made a step forward in the technology of automated poultry inspection.

While machine vision has been successfully applied in fruits and vegetables (Tao, 1994, 1996a,b) and other agricultural industries, its application in the poultry industry, though difficult, is possible with advanced imaging technologies. With joint efforts from the Instrumentation and Sensing Lab of USDA ARS at Beltsville, Maryland, and the Machine Vision and Bioimaging Lab at the University of Arkansas, research was conducted to solve problems in automated vision inspection of poultry carcasses. This research sought to develop imaging techniques for inspecting the internal organs of poultry to identify abnormalities. Focusing on inspecting spleens, this research intended to provide increased detection capabilities for vision systems. At the same time, the new knowledge developed through this research is contributing to the understanding and the development of future advanced technologies in computer-assisted poultry inspections.

Specifically, the objectives of this research were to: (1) develop a spectral imaging method to identify poultry spleen from its surrounding viscera such as livers and intestines; and (2) develop an image processing algorithm that recognizes the spleen in an image and to detect splenomegaly.

## MATERIALS AND METHODS

### IMAGE ACQUISITION

A chamber with controlled lighting was built to acquire images as shown in figure 1. Inside the chamber, a ring fluorescent light (FL) (15 W) and an array of UV lights (eight 20W) surrounded the video camera's lens. Because

---

Article has been reviewed and approved for publication by the Information & Electrical Technologies Division of ASAE.

The authors are **Yang Tao**, *ASAE Member Engineer*, Assistant Professor, **June Shao**, *ASAE Member Engineer*, Research Associate, Biological and Agricultural Engineering Department, **Kirk Skeeles**, Professor and Veterinarian, Poultry Science, University of Arkansas, and **Yud-Ren Chen**, *ASAE Member Engineer*, Research Leader, Instrumentation and Sensing Lab, USDA-ARS, Beltsville, Maryland. **Corresponding author:** Yang Tao, University of Arkansas, 203 Engineering Hall, Fayetteville, AR 72701, phone: 501.575.3402, fax: 501.575.2846, e-mail: <ytao@engr.uark.edu>.

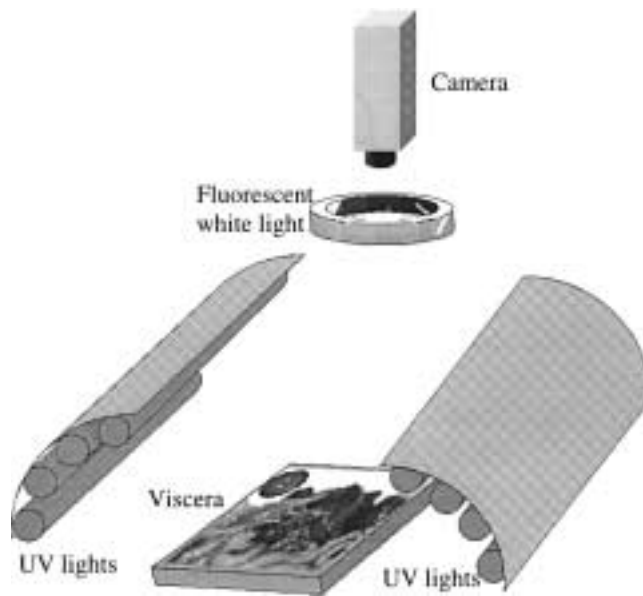


Figure 1—The imaging chamber and lighting configuration.

poultry liver and spleens have the same red color, it is difficult to differentiate these organs using color image processing. It was discovered that UV (central wavelength near 365 nm) lighting was effective to distinguish between the liver and spleen. Due to different biomaterials, the liver and spleen showed distinctive yellow and purple, respectively. A parabolic reflector was mounted above the lights to ensure adequate and evenly distributed illumination. Beneath the camera, a small stand for holding samples was set up at the bottom of the chamber. Without having to move a large amount of machine vision equipment, a video camcorder was used for capturing images. The images were then fed to a PC-hosted image processor for image processing and analysis. Imaging acquisition and algorithms were implemented by a combination of self-designed C/C++ programs, Matrox Imaging Library MIL (Matrox, 1997), and Matlab (1997).

#### EXPERIMENTAL PROCEDURE

The experiment was conducted at the Agricultural Experiment Station Farm of the University of Arkansas at Fayetteville. A total of 52 commercial turkeys was raised in a floor pen facility. When the turkeys were six weeks old, 24 were randomly selected as negative (N) samples while the rest were selected as positive (P) and received individual intravenous injections of turkey propagated Marble Spleen Disease Virus (MSDV) of pheasants. Three days later, each turkey was weighed, euthanized by CO<sub>2</sub> asphyxiation, and necropsied. The viscera of each turkey were removed and placed on the sample holder with spleen faced towards the camera lens. The viscera were alternately imaged under fluorescent and UV lights. After imaging, the spleen was separated and weighed. During the experiment, five out of 52 turkeys were imaged twice with different views for a total of 57 images. A button 22 mm in diameter was placed in the camera's field of view as a size reference for image analysis.

#### IMAGE DETECTION ALGORITHM

Before detecting whether a spleen was enlarged, the image of the spleen first had to be recognized from the surrounding intestines. Under the visible fluorescent light, the spleen and liver shared some color, and the intestines were basically white. Under the UV light, the liver appeared yellow, while the spleen appeared dark purple, making the spleen image recognition easier. However, veins in the mesentery appeared dark purple as well. Because of the complicated background color information displayed, thresholding methods could not be directly applied to the situation. Therefore, a series of image processing and pattern recognition processes had to be developed for spleen recognition and classification. A brief description of the splenomegaly detection algorithm is given below.

**Pixel Statistical Analysis.** Images taken with the camcorder under both visible and UV illuminations alternatively involved six wavebands. Since both color  $C(r, g, b)$  and UV  $U(r, g, b)$  images were taken by the same camera, the images had the same pixel registration (i.e., no pixel shifting). Thus, the two images were merged with each pixel having six attributes indicated as:

$$I [C_r, C_g, C_b, U_r, U_g, U_b] = C(r, g, b) \cup U(r, g, b) \quad (1)$$

where  $r, g,$  and  $b$  denote the pixel values in red, green, and blue frame buffers.  $I$  is a  $640 \times 240 \times 6$  (Horizontal  $\times$  Vertical  $\times$  Band) matrix. Each pixel in  $I$  was considered as a vector with 6 elements, i.e.,  $C_r, C_g, C_b,$  and  $U_r, U_g, U_b$ .

For identifying spleen pixels, spleen characteristics were determined through the statistical measurement of known spleen pixel values. Among the 57 samples (26 N and 31 P), 19 images (9 negatives and 10 positives) were chosen randomly for the derivation of the statistical parameters. From these images, the mean  $\bar{S}_{1 \times 6}$ , covariance  $V_{6 \times 6}$ , and eigenvector  $E_{6 \times 6}$  of spleen pixels were determined. The distance of each pixel  $x, y \in I$  in the vector space was then calculated by:

$$D_{x,y} = I_{x,y} - \bar{S}_{x,y} \quad (2)$$

where  $\bar{S}_{x,y}$  is the mean of spleen pixels and  $D_{x,y}$  is a  $1 \times 6$  vector. The spatial distance calculated from equation 2 provided a quantitative measurement of the difference between a spleen pixel and any other pixels. Generally, if the value of distance  $|D_{x,y}|$  for a given pixel is small or zero, then the given pixel is a spleen pixel. If the distance is large, then it could not be a spleen pixel.

**Linear Transform.** Although the distance could be computed from equation 2, the variance for the spleen pixel values could be very large. It was necessary to normalize the distance in order to find a threshold value that was universal to all images. Linear transform was applied to the distance projected onto the eigenvector. The governing equation of the transform was:

$$D' = D \times (E \times \sqrt{V^{-1}}) \quad (3)$$

where  $D'$  is the resultant difference vector ( $1 \times 6$ ) after the linear transform,  $E$  is the eigenvector, and  $V^{-1}$  is the

inverted covariance matrix ( $V_{6 \times 6}$ ) obtained in statistical image analysis. Based on  $D'$ , a binary image was created by classifying each image pixel as:

$$I_{x,y}^B = \begin{cases} 1 \text{ (spleen) ,} & \text{if } D'_{x,y} < T, D'_{x,y} \in D' \\ 0 \text{ (background) ,} & \text{otherwise} \end{cases} \quad (4)$$

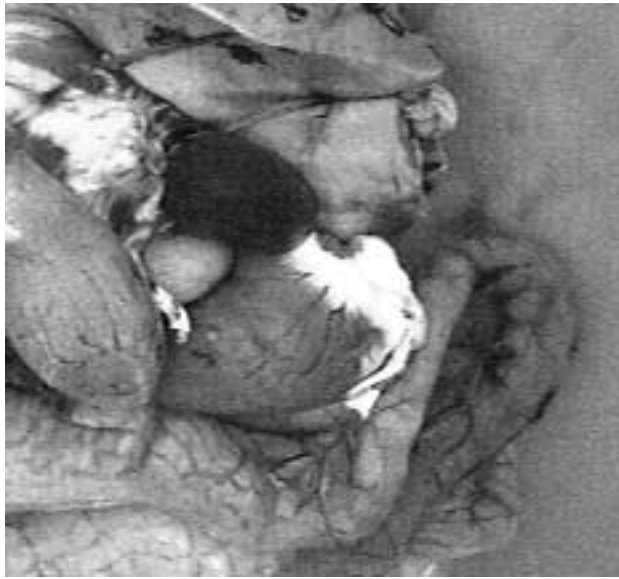
where  $I^B$  is a binary image showing only the extracted spleen, and  $T$  is the threshold vector.

**Morphological Operations.** Morphology was used to further reconstruct the binary spleen image to fill the holes and gaps in the object and to filter out background noises. First, dilation operations were applied to fill gaps between pixels. Then, a labeling operation was performed to obtain the blob of each item in the image. The item having the

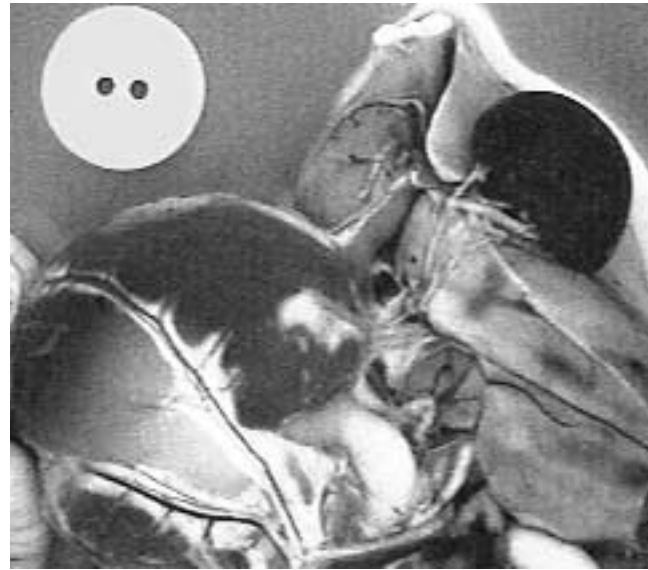
largest blob area was identified as a spleen object. Next, erosion operations were applied to recover the object from the expansion caused by the dilation operation. Finally, if the object had holes, filling operations were performed. After these procedures, the resultant image was binary with the spleen image totally separated from its surroundings.

**Perceptron Classification.** Last, a classification using the perceptron classifier (Gonzalez and Woods, 1992) was used to determine the positive and negative samples. Using variables of spleen area ( $a$ ) and spleen weight ( $w$ ), the decision boundary  $d(a,w)$  implemented by the perceptron is obtained by:

$$d(a,w) = \delta_1 a + \delta_2 w + \delta_0 \quad (5)$$



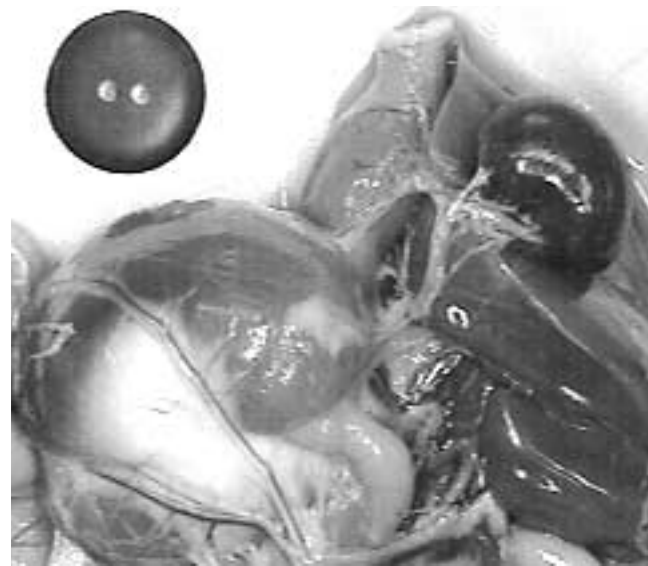
(a) Image of negative sample under UV



(c) Image of positive sample under UV



(b) Image of negative sample under fluorescent light



(d) Image of negative sample under fluorescent light

**Figure 2**—One example of raw images of turkey viscera. Note that the spleens in (a) and (c) show distinctly in intensity from the livers, although both organs have the similar color in the color images (b) and (d). The button in the camera's field of view is used as a size reference.

where  $\delta_1$  and  $\delta_2$  are the weight factors, and  $\delta_0$  is the bias. The perception leaning rule adjusts these weights and bias by minimizing the errors defined as the difference between the calculated and the input actual values. The two classes of normal and abnormal spleen ( $s$ ) were then separated by:

$$s = \begin{cases} \text{abnormal} , & \text{if } d(a,w) \geq 0 \\ \text{normal} , & \text{if } d(a,w) < 0 \end{cases} \quad (6)$$

Since the decision boundary from equation 4 is a linear function, the two classes are separated by a line.

### RESULT AND DISCUSSION

A total of 57 images with 26 negatives and 31 positives was analyzed during the experiment. The results of image processing, body weight and spleen correlation analyses, and classification were collected and analyzed.

#### IMAGE PROCESSING

Figure 2 shows an example of raw images captured under UV and fluorescent lights. Note that in figure 2a, the spleen can be clearly seen as a dark object distinguishable from the surrounding liver, heart, and intestines. Figure 2b shows the color image of the same items, where the spleen

and liver have the same color and intensity. The UV lighting proved effective for imaging identification of spleens.

Figure 3 illustrates the results of the image processing algorithm for image segmentation of spleens. Figure 3a is the resulting image  $I^B$  after the linear transform and segmentation. The morphological operations removed the noisy particles such as from vessels and yielded the image shown in figure 3b. Figures 3c and d show the results when using a positive sample.

Note that the camera had to see the spleen. If the intestines or other organs covered the spleen, it would be hard to be seen. For this experiment, the viscera were placed on the sample plate, and the spleen was oriented in its natural random position facing the camera.

#### STATISTICAL ANALYSIS

Relationships between spleen areas, spleen weight, and body weight were analyzed to correlate spleen size with the detection of positive spleens. Figure 4 shows the plot of spleen weight and body weight. There was a slight correlation between body weight and spleen weight among the positive or negative samples as indicated by their  $R^2$ s of 0.18 and 0.35, respectively. As figure 4 shows, there was a tendency for the spleen weight of the positive samples to be higher than those of negative samples. The same pattern

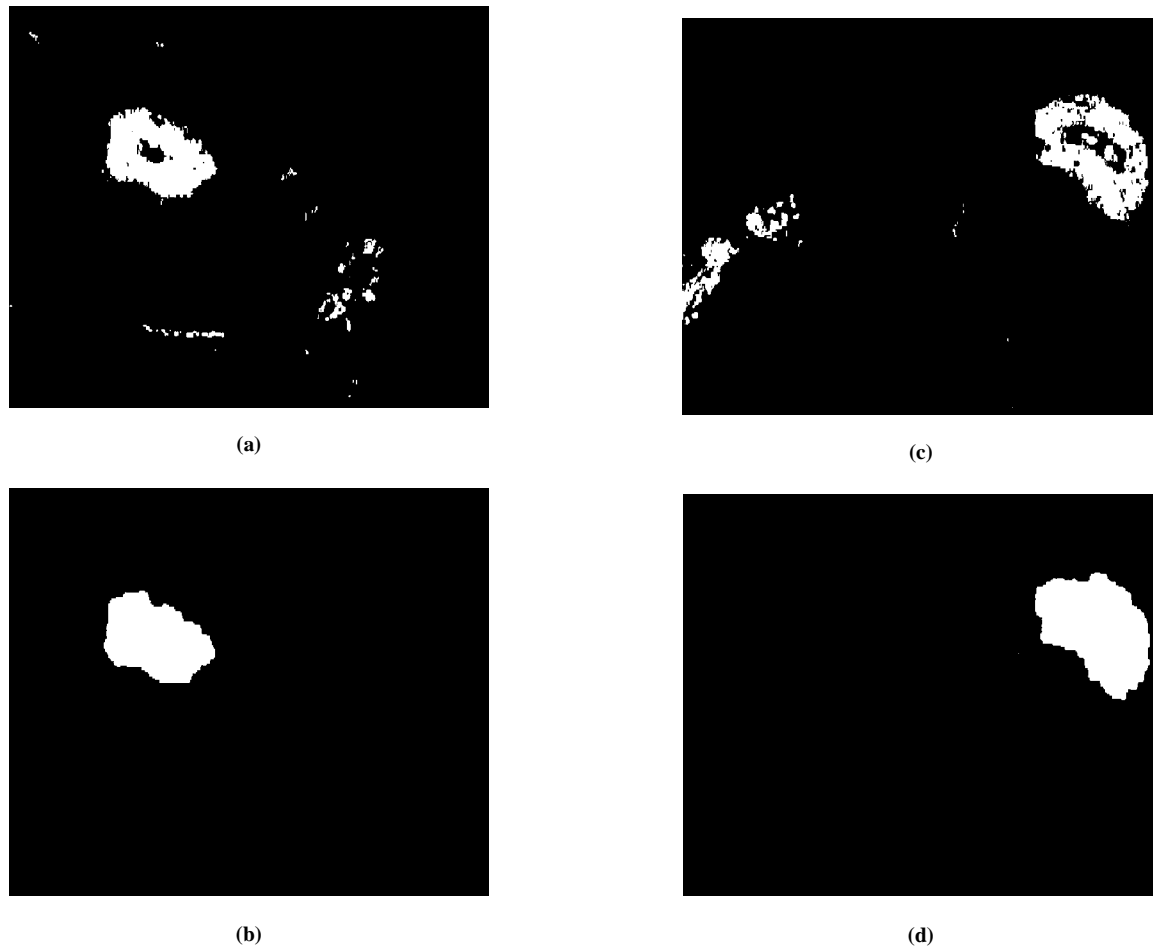
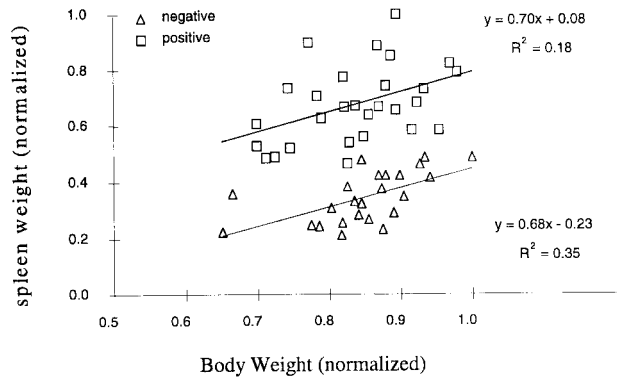


Figure 3—Segmented binary images corresponding to the color images in figure 2. (a) Segmented image after the linear transform (normal spleen), (b) a typical result after the morphological operations on (a). (c) Segmented image after the linear transform (abnormal spleen), and (d) a typical result after the morphological operations on (c).



**Figure 4—Relationship between spleen weight and body weight. The weights were normalized to unity of 2422 g and 7.72 g corresponding to the data maximums, respectively.**

was observed when correlating the spleen area with the body weight as shown in figure 5.

Spleen area and spleen weight correlated very well with  $R^2$  of 0.93, as shown in figure 6. Therefore, the spleen area identified by machine vision can be used to indicate spleen weight for the detection of abnormality. The test of samples showed statistical significance ( $p < 0.001$ ).

To classify positive and negative turkeys, a two-input perceptron method was used. The training set consisted of a total of 38 samples with 18 negatives and 20 positives

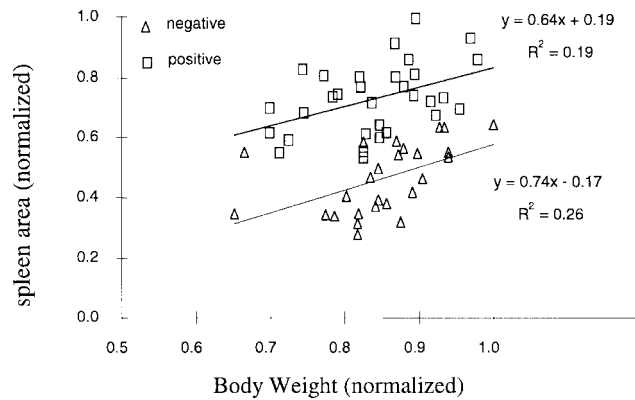


**Figure 5—Relationship between spleen area and body weight. Units normalized to maximums of 517 mm<sup>2</sup> and 2422 g, respectively.**

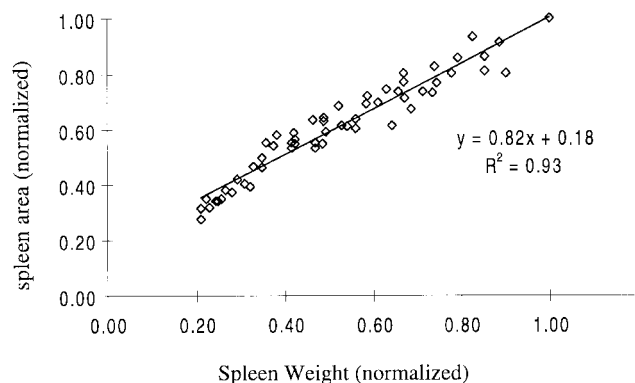


**Figure 6—Relationship between spleen area and spleen weight. The spleen area correlated well to the spleen weight.**

randomly selected from the 57 samples. For the independent testing, a total of 19 samples with 6 negatives and 13 positives was used. Fewer negatives were used because the negative samples were more uniform in size than the positive ones. The classification results are shown in table 1. From the training set, 16 out of 18 negative turkeys and 19 out of 20 positive turkeys were correctly classified, giving the test method an average accuracy rate of 92%. In an independent test set, 6 out of 6 negatives and 12 out of 13 positives were correctly classified, indicating an average accuracy rate of 95%. The misclassified one was not obviously positive and was on the line between positive and negative for splenomegaly. Figure 7 gives the classification results when using perceptron as a classifier of the parameters for the body weight and spleen area. For actual applications, body weight can be easily determined via on-line electronic weighing of individual poultry.

Based on this study, the machine vision methods with UV spectral imaging and identification algorithm for automated checking of internal poultry organs can be added to future online inspection software programs, thus contributing to the knowledge for future advanced technology on computer-assisted inspection.

### CONCLUSION

Detection of poultry diseases from spleen enlargement with computer vision was studied in the research. Through this study, the following conclusions were drawn:

1. The UV imaging method is effective in identifying spleen from surrounding organs and intestines.

**Table 1. Correct classification rates of the perceptron classifier**

Classification	Ratio	Classification Rate (%)
Training		
N	16/18	89
P	19/20	95
Total	35/38	92
Testing		
N	06/06	100
P	12/13	92
Total	18/19	95

N = Native in splenomegaly.  
P = Positive in splenomegaly.

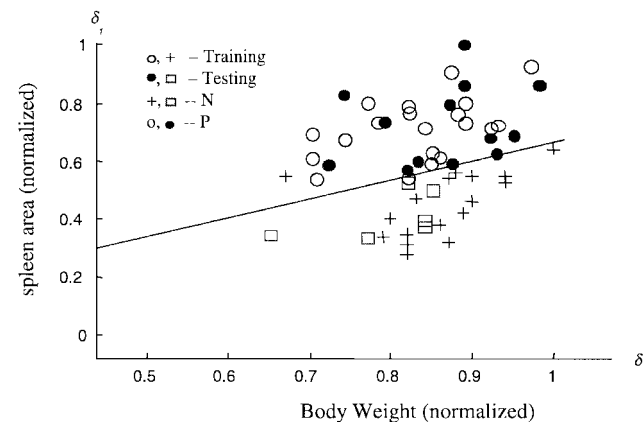


**Figure 7—The result of classification from the two-input perceptron classifier.**

Coupling color imaging with spectral imaging provided useful images for segmentation of targeted objects. The blood vessels on intestines, however, provided background noises that required filtering of images.

2. The image processing algorithm provided effective classification with an overall correct detection rate for abnormal turkeys of 92% for the sample self-training test and 95% in the independent sample test.

**ACKNOWLEDGMENT.** The authors wish to thank the Food Safety Consortium and USDA ARS for the funding support of this research. Thanks to A. Cardarelli, J. Ibarra, R. Bansal, and G. Dwyer for their assistance during the experiment.

## REFERENCES

- Arp, J. H. 1982. Pathology of spleen and liver in turkeys inoculated with *Escherichia Coli*. *Avian Pathology* 11: 263-279.
- Chen, Y. R. N. Nguyen, B. Park, and K. Chao. 1998. Intelligent on-line training and updating of automated poultry inspection system. ASAE Paper No. 98-3047. St Joseph, Mich.: ASAE.
- Clarke, J. K., G. M. Allan, D. G. Bryson, W. Willians, D. Todd, D. P. Mackie, and J. B. McFerran. 1990. Big liver and spleen disease of broiler breeders. *Avian Pathology* 19: 41-50.
- Domermuth, C. H., J. R. Harris, W. B. Gross, and R. T. DuBose. 1978. A naturally occurring infection of chickens with a Hemorrhagic enteritis/marble spleen disease type of virus. *Avian Diseases* 23(2): 479-484.
- Gonzalez, R. C., and R. E. Woods. 1992. *Digital Image Processing*, 595-618. New York, N.Y.: Addison-Wesley Publishing Co., Inc.
- Matlab. 1997. *Software Tool Boxes*. Natick, Mass.: The Mathworks Inc.
- MIL, *Matrox Imaging Library*. 1997. Ver. 5.11. Dorval, Quebec, Canada: Matrox Electronics Ltd.
- Park, B., and Y. R. Chen, M. Nguyen, and H. Hwang. 1996. Characterizing multispectral images of tumorous, bruised, skin-torn, and wholesome poultry carcasses. *Transactions of the ASAE* 39(5): 1933-1941.
- Schat, K. A. 1981. Role of the spleen in the pathogenesis of Marek's disease. *Avian Pathol.* 10: 171-182.
- Tao, Y. 1994. Methods and apparatus for sorting objects by color. U.S. Patent 5,339,963.
- \_\_\_\_\_. 1996a. Methods and apparatus for sorting objects including stable color transformation. U.S. Patent 5,533,628
- \_\_\_\_\_. 1996b. Spherical transform of fruit images for on-line defect extraction of mass objects. *Optical Eng.* 35(2): 344-350.
- Vision, ed. 1998. Cover story "Technology trends: Vision system grades poultry carcasses on-line". *Vision System Designs Magazine* (August).